arXiv:1601.04284v2 [hep-ph] 18 Apr 2016

On the anomalous mass defect of strange stars in the Field Correlator Method

F. I. M. Pereira*

Observatório Nacional, MCTI, Rua Gal. José Cristino 77, 20921-400 Rio de Janeiro RJ, Brazil

(Dated: April 19, 2016)

We investigate general aspects of the mass defects of strange stars in the context of the Field Correlator Method, without magnetic field. The main parameters of the model that enter the corresponding nonperturbative equation of state of the quark gluon plasma are the gluon condensate G_2 and the large distance static $Q\bar{Q}$ potential V_1.

We calculate mass defects of stellar configurations in the central density range $11 < \log \rho_c < 18$. In general, the mass defects are strongly dependent on the model parameters. For a large range of values of G_2 and V_1, we obtain anomalous mass defects with magnitudes around 10^{53} erg , of the same order of the observed energies of gamma-ray bursts and neutrino emissions in SN1987A, and of the theoretically predicted energies of the quark-novae explosions.

Keywords: Strange stars; Mass defects; Strange quark matter; Nonperturbative equation of state.

I. INTRODUCTION

In pioneer works, V. L. Ambartsumyan and G. S. Saakyan considered the question of superdense stellar matter made of a degenerate gas of elementary particles, comprising neutron, protons, hyperons and electrons, at zero temperature [1, 2]. Investigations of internal structures of these compact configurations led to the possibility of stellar transitions of explosive character, from a metastable state to a stable state, with great amounts of liberated energy [3, 4]. These transitions were related to stars with negative (or anomalous) mass

*Electronic address: flavio@on.br

defects characterized by energy excesses with respect to the energies they would have to be (stable) bound systems. Anomalous mass defects were interpreted in terms of a catastrophic additivity violation of the internal energy due to the very intense gravitational fields in the interior of such superdense stellar configurations [5, 6]. An important aspect of these early works rests on the fact that they included the strange baryons - hyperons - in the degenerate (strange) nuclear plasma together with neutrons, protons and electrons.

The baryons being made of quarks, it appeared to be natural to expect unbound quarks to exist in the interior of hyperdense stars. Within this assumption, and in an epoch when the physics of the strong interactions was very incomplete, N. Itoh considered the possibility of hypothetical compact stars made of pure quark matter [7].

With the subsequent developments of the strong interactions theory, new interests came into play connecting the strange nuclear plasma with the physics of quarks. The nuclear interactions within the superdense stellar matter turned out to be described in terms of the baryon constituent quarks. In this context, the strange quark matter (SQM) concept appeared leading to the conjecture of the absolute stability of nuclear matter.

The Bodmer-Terazawa-Witten conjecture [8, 10], which says that the SQM should be the true ground state of the nuclear matter, has attracted a great deal of attention. SQM is a type of quark matter made of approximately equal amounts of u, d and s quarks with a small admixture of electrons in order to maintain the charge neutrality. Its energy per baryon might be lower than the one in ordinary nuclear matter. The SQM properties are of great importance for nuclear physics and astrophysics. In the nuclear physics context, E. Farhi and R. L. Jaffe studied, within the MIT Bag Model (BM), the dependence of the SQM stability on the model parameters, namely, the bag constant B, the strong interactions coupling constant α_c, and the strange quark mass $m_{\rm s}$ [11]. In the astrophysical context, the Bodmer-Terazawa-Witten conjecture has proved to be of great significance for the physics of the strange stars.

Since the 1980's, the properties of strange stars have been considered within the BM [12–15]. In the BM, the quarks enter the equation of state (EOS) as free particles, with the quark confinement being represented by the bag constant B. Another well known model is the Nambu-Jona-Lasinio model [16, 17] used to investigate quark matter properties in compact stars in Refs. [18, 19]. It exhibits chiral symmetry breaking, but the quark confinement is not explicitly included. In alternative investigations, mass density dependent models

were considered to represent confinement in Refs. [20–23]. In a recent work, the Richardson potential [24], which incorporates the asymptotic freedom and linear quark confinement, and also used in Refs. [22, 23], was considered to investigate the SQM in strong magnetic field by the authors of Ref. [25].

Due to the highly nonlinear character of the theory of strong interactions, it was difficult to deal with a definite model of EOS naturally including the quark confinement in terms of the interactions between quarks and antiquarks, and gluons. Thanks to the developments of quantum chromodynamics (QCD), the fundamental theory of the strong interactions, great advances have been made to derive an EOS, including perturbative and/or nonperturbative effects of confinement, to describe quark matter at all finite densities and temperatures.

Recently, Yu. A. Simonov derived, from the first principles, the nonperturbative equation of state (NPEOS) of the quark-gluon plasma in the framework of the Field Correlator Method (FCM) [26]. In the FCM (for a review see Ref. [27] and references therein), the dynamics of confinement is naturally included in terms of the color-electric and color-magnetic correlators. The main parameters of the model that enter the NPEOS are the gluon condensate G_2 and the large distance static $\mathrm{Q\bar{Q}}$ potential V_1, at fixed quark masses and temperature. The model covers the entire phase diagram plane, from the low T and large μ regime to the large T and low μ regime. By connecting the FCM and lattice simulations, at $\mu_c = 0$, the critical temperature turned out to be $T_c \sim 170$ MeV for $G_2 = 0.00682\ \mathrm{GeV}^4$ [28, 29]. Very recently, V. D. Orlovsky and Yu. A. Simonov considered the quark-hadron thermodynamics in the presence of the magnetic field within the FCM [30].

Astrophysical applications of the FCM have been made in the study of neutron stars interiors [31–33] and in the early Universe cosmology [34]. The authors of Ref. [35–37] also applied the FCM to the study of phase transitions in neutron stars matter and to the investigation of the structural properties and stability of hybrid stars.

Recently we applied the FCM to investigate the properties of the strange stars and the SQM stability in Refs. [38, 39]. Of particular significance is the gradual decrease of the widths of the SQM stability windows with the increase of V_1, being zero at $V_1 = 0.5\,\mathrm{GeV}$, the value of V_1 determined from lattice calculations [40]. This aspect is of great importance to investigate the existence of strangelets, mainly in the case of exploding stars with the liberation of matter/energy into the free space, which we here briefly consider (at the end of the present paper).

In the present work, we study the general aspects of the mass defects of strange stars, without crust and magnetic field, within the framework of the FCM. We do not consider the crust here by the same reasons we disregarded it in our previous paper [38]. Crust contributions to the masses of strange stars have been estimated to be $M_{\rm cr} \simeq 2.5 \times 10^{-5}\, M_\odot$ [12], $M_{\rm cr} \simeq (0.9 - 2.3) \times 10^{-5}\, M_\odot$ [41, 42], and $M_{\rm cr} \simeq 3.4 \times 10^{-6}\, M_\odot$ [43]. As we shall see below, the mass defects magnitudes we obtained in the present work are of the order of $10^{53}\,{\rm erg} \simeq 0.056\, M_\odot$, corresponding to $\sim 2.2 \times 10^3\, M_{\rm cr}$, $\sim (2.4 - 2.6) \times 10^3\, M_{\rm cr}$, and $\sim 1.64 \times 10^4\, M_{\rm cr}$, respectively. Crusts are important to investigate compact stars glitches, but we assume here that they are insignificant for the purposes of the present work. On the other hand, in this first attempt to investigate the mass defects of the strange stars, we are interested in the solutions not affected by preferred directions due to magnetic fields, of particular importance to investigate magnetars and soft gamma-ray repeaters [44] as well.

Differently from our strategy adopted in Ref. [38], we here also consider unstable solutions of the hydrostatic equilibrium equations of Tolman-Oppenheimer-Volkov. As a result, depending on the values of the model parameters, G_2 and V_1, solutions with non-negative and/or negative mass defects along a given sequence of stellar configurations are possible. Our aim is to understand the effects of the nonperturbative dynamics of confinement on the binding energies of the strange stars. We give special attention to the anomalous mass defects and, at the end of the paper, briefly comment the corresponding consequences for astrophysical phenomena, such as gamma-ray bursts, supernovae neutrinos or quark-novae explosions.

The present paper is organized as follows. In Sec. II we show the main equations to be used in our calculation. In Sec. III we present the equations to calculate the important quantities of the stellar configurations. In Sec. IV we show the results and in Sec. V we give the final remarks.

II. THE NPEOS AT ZERO TEMPERATURE

In previous works, we outlined the main features of the FCM and showed the equations used to investigate strange stars and strange quark matter properties [38, 39]. So, we now write only the main equations we need here.

For constant V_1, the pressure, energy density and number density of a (one flavor) quark

gas at $T = 0$ are given by

$$p_q^{SLA} = \frac{N_c}{3\pi^2}\left\{\frac{k_q^3}{4}\sqrt{k_q^2+m_q^2} - \frac{3}{8}\,m_q^2\left[k_q\sqrt{k_q^2+m_q^2} - m_q^2\,\ln\left(\frac{k_q+\sqrt{k_q^2+m_q^2}}{m_q}\right)\right]\right\}, \qquad (1)$$

$$\begin{aligned}\varepsilon_q^{SLA} \;=\; & \frac{N_c}{\pi^2}\left\{\frac{k_q^3}{4}\sqrt{k_q^2+m_q^2} + \frac{m_q^2}{8}\,\left[k_q\sqrt{k_q^2+m_q^2} - m_q^2\,\ln\left(\frac{k_q+\sqrt{k_q^2+m_q^2}}{m_q}\right)\right]\right. \\ & \left. +\; \frac{V_1}{2}\,\frac{k_q^3}{3}\right\} \end{aligned} \qquad (2)$$

and

$$n_q^{SLA} = \frac{N_c}{\pi^2}\,\frac{k_q^3}{3}\,, \qquad (3)$$

where

$$k_q = \sqrt{(\mu_q - V_1/2)^2 - m_q^2}\,, \quad (q = \mathrm{u,d,s})\,, \qquad (4)$$

and $N_c = 3$ is the color number; and SLA indicates the single line approximation considered in Ref. [26]. When $V_1 = 0$, the ordinary Fermi momentum k_F of a free quark gas is recovered in Eq. (4). The additional term $(V_1/2)k_q^3/3$ in Eq.(2) comes from the large distance static $Q\bar{Q}$ potential V_1.

Inside a strange star, the weak interaction reactions $d \to u + \mathrm{e} + \bar{\nu}_\mathrm{e}$, $\mathrm{e} + u \to d + \nu_\mathrm{e}$, and $s \to u + \mathrm{e} + \bar{\nu}_\mathrm{e}$, $u + \mathrm{e} \to s + \nu_\mathrm{e}$ imply weak equilibrium between quarks, whereas neutrinos and anti-neutrinos leave the star without interaction and their chemical potentials can be set to zero. In this case, the chemical equilibrium is given by

$$\mu_d = \mu_u + \mu_\mathrm{e} \quad \text{and} \quad \mu_s = \mu_d\,. \qquad (5)$$

The overall charge neutrality requires that

$$\frac{1}{3}(2n_u^{SLA} - n_d^{SLA} - n_s^{SLA}) - n_\mathrm{e} = 0\,, \qquad (6)$$

where n_i is the number density of the particle i =u,d,s,e.

To calculate stellar configurations, with charge neutrality and chemical equilibrium, the total pressure and energy density, including electrons are given by

$$p = \sum_{q=u,d,s} p_q^{SLA} - \Delta|\varepsilon_\mathrm{vac}| + p_\mathrm{e}\,, \qquad (7)$$

$$\varepsilon = \sum_{q=u,d,s} \varepsilon_q^{SLA} + \Delta|\varepsilon_{\rm vac}| + \varepsilon_{\rm e} \ , \tag{8}$$

where

$$\Delta|\varepsilon_{\rm vac}| = \frac{11 - \frac{2}{3}N_f}{32}\Delta G_2 \ , \tag{9}$$

is the vacuum energy density difference between confined and deconfined phases and N_f is the number of flavors. The difference between the values of the gluon condensate, as predicted by lattice calculations, is $\Delta G_2 = G_2(T < T_c) - G_2(T > T_c) \simeq \frac{1}{2}G_2$ [28, 29].

In order to obtain the numerical correspondence between FCM and BM, we make the identifications: $\Delta|\varepsilon_{\rm vac}| = B$ and $V_1 = 0$. However, we here emphasize that $\Delta|\varepsilon_{\rm vac}|$ is essentially a nonperturbative quantity. For the quark masses, we use $m_u = 5$ MeV, $m_d = 7$ MeV and $m_s = 150$ MeV. The corresponding equations for the degenerate electron gas are similar to the ones above and can be easily obtained by making the changes: $N_c \to 1$, $V_1 \to 0$, $\mu_q \to \mu_{\rm e}$ and $m_q \to m_{\rm e}$. We use the same numerical strategy adopted in Ref. [38] to calculate strange stars configurations.

III. COMPACT STARS CONFIGURATIONS

Compact stars configurations are calculated by numerical integration of the Tolman-Oppenheimer-Volkov hydrostatic equilibrium equations [45–47]. Of particular importance here is the total gravitational mass of a compact star,

$$M = 4\pi \int_0^R \varepsilon(r)\, r^2 dr \ , \tag{10}$$

which is the mass that governs the Keplerian orbital motion of the distant gravitating bodies around it, as measured by external observers. The proper mass is given by

$$M_P = \int_0^R \varepsilon(r)\, dV(r) \ , \tag{11}$$

where $dV(r) = 4\pi[1 - 2Gm(r)/r]^{-1/2}\, r^2\, dr$ and $m(r)$ is the mass within a sphere of radius r. The proper mass is the sum of the mass elements $dm(r) = \varepsilon(r)\, dV(r)$ measured by a local observer. The baryonic mass (also called rest mass) of a star is $M_A = N_A m_A$, where

$$N_A = \int_0^R n_A(r)\, dV(r) \tag{12}$$

is the number of baryons within the star, m_A is the mass of the baryonic specie A, and

$$n_A = \frac{1}{3}(n_u^{SLA} + n_d^{SLA} + n_s^{SLA}) \tag{13}$$

is the baryon number density. The baryonic mass has a simple interpretation: it is the mass that the star would have if its baryon content were dispersed at infinity. In the case of the strange stars (because of the quark confinement), N_A is the equivalent number of baryons (not quarks). There is some freedom to choose the baryonic mass. In earlier texts, the baryonic mass was taken as the mass $m_{\rm H}$ of the hydrogen atom [3]; the $^{56}{\rm F_e}$ mass per baryon $m_0 \equiv m(^{56}{\rm Fe})/56$ [14, 47–50]; or the neutron mass m_n [4, 5, 38, 46]. We here assume $m_A = m_n$, as in Ref. [38]. Comparison of some results with respect to m_0 is also made below.

Let us now consider the mass defect of a compact stars we are concerned in the present work. The *incomplete mass defect* or, for short, the *mass defect* is the difference $\Delta_2 M = M_A - M$ (which in our notation[1] is minus the binding energy E_b defined in Refs. [46, 47]). It corresponds to the energy released to aggregate from infinity the dispersed baryonic matter. A stellar configuration is stable if $\Delta_2 M > 0$ (normal mass defect) and unstable if $\Delta_2 M < 0$ (anomalous mass defect).

IV. RESULTS

We calculated sequences of strange star configurations for central densities in the range $11 < \log \rho_c < 18$. In general, the forms of the sequences and the respective mass defects of stellar configurations strongly depend on the values of the model parameters. A typical example is shown in Fig. 1, for $G_2 = 0.006\,{\rm GeV}^4$ [26] and $V_1 = 0$. The stellar sequence present three branches delimited at the labeled points 1 and 2, where the solid and dashed curves cross itself, and in which $M = M_A$, as shown in panel (a). In the intermediate branch we have $M < M_A$, required by the stability conditions against transition to diffuse matter. We have $M > M_A$ at densities $\sim 10^{15}{\rm g\,cm^{-3}}$ in the first branch[2], and $> 5.5 \times 10^{16}{\rm g\,cm^{-3}}$ in the third branch.

An investigation of strange stars within BM, for the values of the bag constant in the range $50\,{\rm MeV\,fm^{-3}} \leq B \leq 70\,{\rm MeV\,fm^{-3}}$, showed the absence of the anomalous mass defect

[1] We here follow the notation according to Refs. [1, 2, 4, 49, 50].
[2] Not well visible in the scales of panels (a) and (b), but visible in panel (c).

in strange stars [50]. Anomalous mass defects does not have been obtained because of the low used values of B, which numerically correspond (in our calculation with $V_1 = 0$) to lower values of $\Delta|\varepsilon_{\rm vac.}|$ (or G_2). In fact, in the FCM, for $V_1 = 0$ and $G_2 \lesssim 0.0043\,{\rm GeV}^4$, the stellar configurations present normal mass defects. To obtain, within the BM, stellar configurations with anomalous mass defects in the first branch we need $B > 78.7\,{\rm MeV\,fm}^{-3}$ (corresponding to $G_2 > 0.0043\,{\rm GeV}^4$). To obtain anomalous mass defects both in first and in third branches, we need $B \gtrsim 110\,{\rm MeV\,fm}^{-3}$ (corresponding to $G_2 \gtrsim 0.006\,{\rm GeV}^4$). Values of B between $150\,{\rm MeV\,fm}^{-3}$ and $170\,{\rm MeV\,fm}^{-3}$ were considered to explain the time elapsed between the transition from a metastable neutron star generated by a supernova explosion and the new collapse generating the delayed gamma-ray burst by the authors of Ref. [51]. Moreover, higher values of B up to $337\,{\rm MeV\,fm}^{-3}$ and $353\,{\rm MeV\,fm}^{-3}$ were considered, but to calculate at nonzero temperatures the quark deconfinement in the cores of protoneutron stars [53].

Of particular interest is the dependence of M with the number of baryons N_A shown in panel (b), with the labels 1 and 2 as in panel (a). The cusp is at the maximum value of M, where N_A is also maximum[3]. Also shown is the M_A plot with its upper "endpoint"[4] at the maximum M_A. In the upper part of the M vs. N_A plot (above 1) the situation is analogous to that of neutron stars in that $dM/dN_A < m_A$ everywhere on the corresponding plot segments; $M < M_A$ in the second branch and $M > M_A$ in the third branch [47]. However, a fact that was not observed in earlier works (because of the EOS used) is that $M > M_A$ in the first branch (below 1). Moreover, the slope starts with $dM/dN_A > m_A$, turns to $dM/dN_A = m_A$ at an intermediate point and then to $dM/dN_A < m_A$ as N_A grows. In contrast with neutron star configurations, we have here a situation with $M > M_A$ and $dM/dN_A > m_A$ apparently not obeying the $dM/dN_A = m_A\,[1 - 2GM/R]^{1/2}$ prescription [48]. This is a characteristic feature of the anomalous mass defects occurring in the first branch making evident the role of the confinement effects.

Panel (c) shows the mass defect as function of $M/M_\odot$ with the delimiters 1 and 2 as in panels (a) and (b). Differently from Refs. [1, 2, 4], the mass defects are also negative in the

[3] See footnote 2 in Ref. [38].

[4] In reality, it is not an endpoint because, at the upper point, the plot comes back along the same straight line.

first and third branches[5]. For the given values of the parameters G_2 and V_1, the maximum $\Delta_2 M$ magnitude is of the order of $\sim 0.15 \times 10^{53}\,\mathrm{erg}$ at $M \sim 0.26\,M_\odot$ in the first branch, and $\sim 0.3 \times 10^{53}\,\mathrm{erg}$ at the endpoint of the third branch at $M \sim 0.9\,M_\odot$.

A variety of behaviors can be obtained by the variation of the model parameters. Some typical examples are shown in Fig. 2. Panels (a) and (b) show the case $M < M_A$ for which the mass defect has the normal sign ($\Delta_2 M > 0$) everywhere along the sequence of stellar configurations, as in panel (c). Panels (d) and (e) correspond to the limit $M = M_A$ at the maximum mass, but with anomalous mass defects at all the other points of the stellar sequence with $M > M_A$, as depicted in panel (f). Finally, panels (g) and (h) show the case $M > M_A$, so $\Delta_2 M < 0$ at all points along the sequence, as in panel (i). Notice the pronounced confinement effects on the stellar sequences in panels (d)-(f) and (g)-(i). This general overview shows us that anomalous mass defects can (in principle) be obtained for arbitrary values of the model parameters. If G_2 is low, V_1 must be increased in order to yield anomalous mass defect; if V_1 is low, G_2 must grow in order to produce the same effect. As it was stated above, new results emerge with the use of the NPEOS provided by the FCM: for V_1 in the range $0 \leq V_1 \leq 0.5\,\mathrm{GeV}$, stellar configurations with anomalous mass defects are possible not only in the first branch but also in the third branch, at densities larger than the nuclear one. Merely illustratively, we also show the proper mass M_P which is greater than both M and M_A.

On account of the above features, in the energy range we are considering, the $G_2 - V_1$ plane can be divided in three different regions according to the signs of $\Delta_2 M$ as shown in Fig. 3. In doing so, we obtain three regions. The first region, A, with $\Delta_2 M > 0$ everywhere on the sequence. In the second region, B, with features analogous to those in Fig. 1, both normal and anomalous mass defects are present in the same stellar sequence. Finally, the third region, C, with $\Delta_2 M < 0$ along all the sequence of stellar configurations. The idea of Fig. 3 serves to predict values of V_1 and G_2 according to the types of the stellar configurations and the respective mass defects we want.

A star with anomalous mass defect has an exceeding stored energy with respect to the one needed to form a compact stable bound system. In principle, in a given sequence of

[5] From now on, we do not mention the value of $\Delta_2 M$ at the origin because it is obviously zero as M , M_A and $N_A \to 0$, unless stated otherwise.

stellar configurations, any star with $\Delta_2 M < 0$ might explode or implode (for example, in the presence of certain perturbations) with a liberation of an enormous amount of energy. In the case of explosion, the scattered matter will have a nonzero kinetic energy at infinity.

On the other hand, it is well known that stellar configurations obtained from Tolman-Oppenheimer-Volkov equations are stable if $dM/d\rho_c > 0$, corresponding to the stars in the ascending branch of the stellar sequence, as in panel (a) of Fig. 1. In the descending branch, where $dM/d\rho_c < 0$, the stellar configurations are unstable against gravitational collapse to black hole. Then, a stable configuration pass from stability to instability at the peak of the sequence where M, M_A and N_A attain their maximums (for a detailed analysis of stability, see Refs.: [46, 48]). Hence, the investigation of the mass defects in this transition limit may be of particular interest.

Among the many possibilities, as the ones shown in Figs. 1 and 2, let us now consider (both normal and anomalous) mass defects at the maximum masses of the stellar configurations, as depicted in Fig. 4. The plots cover a large area in the $G_2 - \Delta_2 M$ plane, as shown in panel (a). It is evident that nonnegative values of $\Delta_2 M$ occur for $G_2 \lesssim 0.00927\,\mathrm{GeV}^4$, which gives the vacuum energy density $\Delta|\varepsilon_{\mathrm{vac}}| \lesssim 0.0013\,\mathrm{GeV}^4 \simeq 170\,\mathrm{MeV\,fm}^{-3}$. Above these values of G_2 (or $\Delta|\varepsilon_{\mathrm{vac}}|$), $\Delta_2 M$ is anomalous whatever the values of V_1 may be between zero and $0.5\,\mathrm{GeV}$.

At $V_1 = 0.5\,\mathrm{GeV}$, the anomalous mass defect attains its maximum magnitude at $\simeq 6.27 \times 10^{53}\,\mathrm{erg}$, but for $G_2 \simeq 0.000625\,\mathrm{GeV}^4$, corresponding to a strange star with $M \simeq 1.59\,M_\odot$ and $M_A = 1.24\,M_\odot$. In the FCM framework, this is the maximum allowed energy to be liberated in a possible explosion. Such a star has a fraction of stored energy around $|\Delta_2 M|/M \sim 22\,\%$, but it is not a maximum. For instance, in the range $0 \leq G_2 \lesssim 0.0095\,\mathrm{GeV}^4$, the fractions of the mass excess may be as large as $\sim 25\,\%$ for $V_1 = 0.3\,\mathrm{GeV}$ and $G_2 = 0.006\,\mathrm{GeV}^4$; $\sim 34\,\%$ for $V_1 = 0.4\,\mathrm{GeV}$ and $G_2 = 0.007\,\mathrm{GeV}^4$; and $\sim 42\,\%$ for $V_1 = 0.5\,\mathrm{GeV}$ and $G_2 = 0.0095\,\mathrm{GeV}^4$. Concerning the masses in the above range of the anomalous mass defects, along the $V_1 = 0.5\,\mathrm{GeV}$ curve, they vary from $M \simeq 4.7\,M_\odot$ (maximum at the $\Delta_2 M = 0$ limit) at $G_2 = 2.5 \times 10^{-5}\,\mathrm{GeV}^4$ to $M \simeq 0.63\,M_\odot$ at $G_2 = 0.0095\,\mathrm{GeV}^4$. For other values of V_1 the masses assume intermediate values.

As G_2 increases, the apparent "convergence" of the curves led us (speculatively) to extrapolate our calculations to $G_2 = 0.1\,\mathrm{GeV}^4$, beyond the limits of the analysis made in Ref. [52], as shown in panel (b). As a result we obtained a slightly ascending tail with

$\Delta_2 M \simeq -2.7 \times 10^{53}\,\mathrm{erg}$ at the endpoint. Along this tail the masses vary, for example, from $M \simeq 0.49\,M_\odot$ at $V_1 = 0$ and $G_2 = 0.05\,\mathrm{GeV}^4$ to $M \simeq 0.25\,M_\odot$ at $V_1 = 0.5\,\mathrm{GeV}$ and $G_2 = 0.1\,\mathrm{GeV}^4$. For the intermediate values of V_1 the masses are also intermediate. The mass excess fractions may be as large as $\sim 33\,\%$ for $V_1 = 0$ and $G_2 = 0.05\,\mathrm{GeV}^4$; $\sim 52\,\%$ for $V_1 = 0.3\,\mathrm{GeV}$ and $G_2 = 0.08\,\mathrm{GeV}^4$; and $\sim 60\,\%$ for $V_1 = 0.5\,\mathrm{GeV}$ and $G_2 = 0.1\,\mathrm{GeV}^4$. Extending (now, arbitrarily speculatively) our extrapolation to $G_2 = 1\,\mathrm{GeV}^4$, the anomalous mass defects along the tail are not greater than $-1.2 \times 10^{53}\,\mathrm{erg}$. At $G_2 = 1\,\mathrm{GeV}^4$, the masses vary from $M \simeq 0.11\,M_\odot$ at $V_1 = 0$ to $M \simeq 0.09\,M_\odot$ at $V_1 = 0.5\,\mathrm{GeV}$; the excess fractions changing from $\sim 68\%$ to $\sim 74\%$, respectively.

For large values of G_2 (say, $G_2 > 0.07\,\mathrm{GeV}^4$), the curves concentrate in a narrow band. Then, it should be very difficult (or a very accurate determination, as for instance in gamma-ray bursts observations, should be required) to extract, from the $|\Delta_2 M|$ measurements around $\sim 3 \times 10^{53}\,\mathrm{erg}$, reasonable estimates for V_1 and/or G_2. By the way, as a general case in the $G_2 - \Delta_2 M$ plane, we need an additional measurement to determine unambiguously the model parameters G_2 and V_1. For the sake of comparison with the BM, the open circles along the $V_1 = 0$ curve correspond to the values of B used in Refs. [12–15, 49–51].

Here, a curious fact comes from the supernova SN1987A. The neutrino signals were detected at Kamiokande II [54] and at IMB [55]. The total energy of the observed neutrinos was found to be $\sim 3 \times 10^{53}\,\mathrm{erg}$. It was pointed out that one signal might have been originated in the formation of a neutron star after the supernova explosion and the other signal in a possible formation of a strange star [50]. It is inquisitive that the values of $|\Delta_2 M|$ along the tail in panel (b) of Fig. 4 are roughly coincident with the energy of the SN1987A neutrinos. Also, of similar magnitudes are the gamma-ray bursts GRB970828 with $\sim 2.7 \times 10^{53}\,\mathrm{erg}$ [51] and GRB971214 with an inferred energy loss of $\sim 3 \times 10^{53}\,\mathrm{erg}$ [56] (assuming isotropic emissions). Hence, measurements of $|\Delta_2 M|$ around these energy values may be of particular importance.

Finally, within our freedom to choose the value of m_A, we performed our investigation assuming $m_\mathrm{A} = m_\mathrm{n}$. Taking into account that m_A enters the expression of M_A as an external factor multiplying N_A in Eq. 12, the conversion formula given $\Delta_2 M$ in terms of

$m_0 = m(^{56}\mathrm{F_e})/56$ is

$$\begin{aligned} \Delta_2 M(^{56}\mathrm{F_e}) &= \Delta_2 M + (\eta - 1) M_A \\ &= \Delta_2 M - 0.175 \times 10^{53} (M_A/M_\odot)\,, \end{aligned} \tag{14}$$

where $\eta = m_0/m_n \simeq 0.9902$ and $M_\odot \simeq 1.988 \times 10^{33}\mathrm{g} \simeq 1.787 \times 10^{54}\mathrm{erg}$. In Fig. 5, the curves corresponding to $m_A = m_0$ are slightly shifted with respect the ones for $m_A = m_\mathrm{n}$. In the context of baryonic stars, interesting comments about the possibility of states with $\Delta_2 M < 0$ be reached by the release of nuclear energy, for the case of rarefied hydrogen and the case of rarefied iron vapor dispersed at infinity, are made in Ref.: [47].

V. FINAL REMARKS

Previous investigations showed that the FCM provides new possibilities for the investigation of compact stellar configurations [31–33, 35–38]. In the present work, we considered the general aspects of the mass defects of strange stars within the FCM without magnetic field, with special emphasis on the anomalous mass defects. Concerning the magnitudes of the anomalous mass defects, our results are consistent with the estimated electromagnetic energies of the gamma-ray bursts, varying from $0.07 \times 10^{53}\,\mathrm{erg}$ in GRB970508 to $5 \times 10^{53}\,\mathrm{erg}$ in GRB011211 (assuming isotropic emission), given in Table 1 of Ref. [51] , and the theoretical energy predictions of quark-nova explosions [57].

Since quarks are not freely observed, a strange star in an explosion process must liberate its energy excess as neutrinos, gamma-rays, gravitational waves, or other forms of matter/energy. If the ejected matter is made of hadrons, then a transformation to the hadron phase is needed in order to disperse the hadronic content to infinity. Another possibility would be the energy release in the form of strangelets [10–12]. Strangelets are lumps of self-bound matter containing as few as a thousand of u, d and s quarks. The question of strangelets was considered in Ref. [58]. It was argued that a disruption of a strange star would contaminate the Galaxy with an exceeding density of strangelets with respect to that required to transform neutron stars into strange stars [59]. However, in order to such a contamination takes place, it is expected that the strangelets must survive a long time, hence the need to investigate the SQM stability.

Very recently, we considered for several values of V_1 the behavior of the stability win-

dows of the SQM (with respect to the $^{56}F_{\rm e}$ nucleus) with chemical equilibrium and charge neutrality (cf. panel (a) of Fig. 3 in Ref.: [39]). Within the same line, we determined here the value of V_1 in order to give a zero stability window at the s-quark mass $m_s = 0.15\,{\rm GeV}$. As a result we obtained $V_1 = 0.33\,{\rm GeV}$, as shown in panel (a) of Fig. 6, which also includes (for comparison) the nonzero windows at $V_1 = 0$, 0.1 GeV and 0.2 GeV. At the given s-quark mass (dashed horizontal line), the stability windows are zero in the range $0.33\,{\rm GeV} \leq V_1 \leq 0.5\,{\rm GeV}$. On the other hand, the largest window width occurs at $V_1 = 0$ for any s-quark mass $m_s \geq 0$, being maximum at $m_s = 0$. Then, it should be interesting to express the SQM stability, at a given m_s, in terms of a relative stability, which we crudely estimated by considering three different possibilities. If for each value of V_1, we compare the width of the stability window at $m_s = 0.15\,{\rm GeV}$ with the corresponding (maximum) value at $m_s = 0$, we observe that the SQM stability gradually decreases from about 53 % at $V_1 = 0$ to zero at $V_1 = 0.33\,{\rm GeV}$, as shown in panel (b). On the other hand, if for each value of V_1, we compare the width of the stability window at $m_s = 0.15\,{\rm GeV}$ with the one at $V_1 = 0$ (at the same $m_s = 0.15\,{\rm GeV}$), the SQM stability also decreases very rapidly from 100 % at $V_1 = 0$ to zero at $V_1 = 0.33\,{\rm GeV}$ (short dashed line). Finally, if for each value of V_1, we compare the width of the stability window at $m_s = 0.15\,{\rm GeV}$ with the largest one (at $m_s = 0$ and $V_1 = 0$) we observe the fastest rate of stability decrease (long dashed line). The relative stabilities are $\lesssim 40\%$ at $V_1 \simeq 0.1\,{\rm GeV}$; $\lesssim 20.5\%$ at $V_1 \simeq 0.2\,{\rm GeV}$ and $\lesssim 2.5\%$ at $V_1 \simeq 0.3\,{\rm GeV}$. Then, in this aspect, for reasonable values V_1 it is unlikely that the strangelets ejected from strange star explosions should survive so long (before they decay) to arrive on Earth or other place of the Galaxy. These results appeared to be in accordance with terrestrial experiments at RHIC which have not confirmed the existence of the SQM nor proved that it does not exists [60–62].

In an investigation relating the gamma-ray bursts to a second explosion after the (first) supernova explosion, it was pointed out that the main difficulties of the model were to explain the causes of the second explosion and the time elapsed between the first explosion and second explosion [63]. In this regard, another interesting aspect to be considered would be the connection between the anomalous mass defects and stellar instabilities. Merely speculatively, it appears to be reasonable to expect that the greater the magnitude of the anomalous mass defect is, the greater might be the instability of a strange star configuration. Correspondingly, the lower might be the time interval between the first (supernova)

explosion and the second (quark-nova) explosion. However, such an investigation should require detailed studies of the internal structure as well as internal processes of the strange stars, that merit to be considered elsewhere, in the author's opinion.

Finally, although the main aim of the present work is the study of the mass defects of the strange stars, with emphasis on the anomalous mass defects, let us here consider some general aspects concerning the low-mass strange stars as well as their importance for further investigations in the FCM.

In Sec. IV, we showed that low-mass strange stars with anomalous mass defects are possible in the first branch, as in Fig. 1. These stars are important for both theoretical and observational investigations. For $M > M_{\odot}$, strange stars and neutron stars with the same mass present similar radii, but for $M < M_{\odot}$ their radii are markedly different [12, 64]. Another feature is that the strange stars, being more compact, have lager surface redshifts than the ones for neutron stars [65]. It would be possible to distinguish strange stars and neutron star by radii direct measurements of low mass pulsar-like stars by observations from X-ray satellites [66](and references therein). The identification of strange stars with $M \lesssim 0.1 M_{\odot}$ can show us if they are bare stars given that their radii are much lower than the ones for stars with crust, in the low mass limit [67].

Due to the fact that the quarks and anti-quarks are held together by the strong interaction forces, the strange stars are self-bound systems, even in the absence of gravitation, whereas neutron stars are not. In the low-mass regime, the mass-radius relations of strange stars have been well represented by the use of the approximated BM equation of state in the $m_q \to 0$ (q=u,d,s) limit,

$$p = \frac{1}{3}(\varepsilon - 4\,B) \tag{15}$$

which was used to calculate mass-radius relations in Refs. [10, 12].

The low-mass strange stars obey the $M \propto R^3$ dependence which can be easily explained within the BM. For $M \lesssim 0.3 M_{\odot}$, the gravitational pull becomes small compared to the contribution of the vacuum energy density represented by the bag constant B. Inside the star, due to the high degree of incompressibility of the SQM, the energy density is nearly constant (cf. Fig. 1 in Ref. [12] or Fig. 8.6 in Ref. [65]. In this case, the Newtonian approximation suffices to calculate the mass of the strange star as being $M \simeq (4\pi/3) R^3\, \varepsilon$.

In the FCM, the corresponding simplified NPEOS is (from Eqs. (1)-(9)) given by

$$\begin{aligned} p &= \frac{1}{3}\left[\varepsilon - \frac{3}{2}V_1 n_A - 4\Delta|\varepsilon_{\rm vac}|\right] \\ &= \frac{1}{3}\left[\varepsilon - \frac{3}{2}V_1 n_A - \frac{9}{16}G_2\right]. \end{aligned} \tag{16}$$

There is here an important point to be addressed. Apart from the low-mass strange stars in the first branch, where the use of Eq. (16) is valid, we also have sequences of stellar configurations with maximum masses in the low-mass region (as in panel (g) of Fig. 2) where Eq. (16) is not generally valid, even when $M_{\rm max} \simeq 0.3\,M_\odot$. For instance, in the region of anomalous mass defects, corresponding to $0 \leq V_1 \leq 0.5\,{\rm GeV}$ and G_2 in the extrapolated tail ($0.02\,{\rm GeV}^4 \lesssim G_2 \lesssim 0.1\,{\rm GeV}^4$) in Fig. 4 (panel (b)), the maximum masses are in the region $0.2\,M_\odot < M_{\rm max} < 0.5\,M_\odot$. However, as a part of a next work, we say in advance that it is not generally true that Eq. (16) is an appropriate approximation [68]. According to our preliminary exact numerical calculations, depending on the values of V_1 and G_2, inside a star with $M = M_{\rm max}$ in the low-mass region it is not mandatory for the energy density $\varepsilon(r)$ be nearly constant in order to allow for the usage of the Newtonian approximation. In this case, it appears that the concept of low-mass strange stars must be taken as meaning $M < M_{\rm max}$ rather than $M < M_\odot$. Correspondingly, we expect that these features may imply interesting consequences to the anomalous mass defects.

ACKNOWLEDGMENTS

I would like to thank J. S. Alcaniz, R. Silva and A. P. Santos. This work was done with the support provided by the Ministério da Ciência , Tecnologia e Inovação (MCTI).

[1] V. A. Ambartsumyan, G. S. Saakyan, Sov. Astron -AJ 4 (1960) 187.

[2] V. A. Ambartsumyan, G. S. Saakyan, Sov. Astron -AJ 5 (1962) 601.

[3] V. A. Ambartsumyan, G. S. Saakyan, Sov. Astron -AJ 5 (1962) 779.

[4] G. S. Saakyan, Yu. L. Vartanyan, Sov. Astron.-AJ 8 (1964) 147.

[5] V. A. Ambartsumyan, G. S. Saakyan, Astrofizika 1 (1965) 7.

[6] G. S. Saakyan, in Problemes de la Cosmogonie Contemporaine (Ed.: V. A. Ambartsumyan), Editions MIR, Moscou, 1971.

[7] N. Itoh, Prog. Theor. Phys. 44 (1970) 291.

[8] A. R. Bodmer, Phys. Rev. D4 (1971) 1601.

[9] H. Terazawa, INS-Report-336 (INS, University of Tokyo, Tokyo) May, 1979.

[10] E. Witten, Phys. Rev. D30 (1984) 272.

[11] E. Farhi, R. L. Jaffe, Phys. Rev. D30 (1984) 2379.

[12] C. Alcok, E. Farhi, A. Olinto, Astrophys. J. 310 (1986) 261.

[13] P. Haensel, J. L. Zdunik, R. Schaeffer, Astron. Astrophys. 160 (1986) 121.

[14] Yu. L. Vartanyan, A. R. Arutyunyan, A. K. Grigoryan, Astron. Lett. 21 (1995) 122.

[15] K.Kohri, K. Iida, Sato, K., Prog. Theor. Phys. Suppl. 151 (2003) 181.

[16] Y. Nambu, G. Jona-Lasinio, Phys. Rev. 122 (1961) 345.

[17] Y. Nambu, G. Jona-Lasinio, Phys. Rev. 124 (1961) 246.

[18] D. P. Menezes, C. Providência, Phys. Rev. C68 (2003) 035804.

[19] D. P. Menezes, C. Providência, Braz. J. Phys. 34 (2004) 724.

[20] O. G. Benvenuto, G. Lugones, Phys. Rev. D51 (1995) 1989.

[21] G. Lugones, O. G. Benvenuto, Phys. Rev. D52 (1995) 1276.

[22] M. Dey, I. Bombaci, J. Dey, S. Ray, B. C. Samanta, Phys. Lett. B438 (1998) 123.

[23] M. Dey, I. Bombaci, J. Dey, S. Ray, B. C. Samanta, Phys. Lett. B467 (1999) 303, Erratum.

[24] J. L. Richardson , Phys. Lett. B82 (1979) 272.

[25] M. Sinha, Xu-Guang Huang, A. Sedrakian , Phys. Rev. D88 (2013) 025008.

[26] Yu. A.Simonov, Ann. Phys. 323 (2008) 783.

[27] A. Di Giacomo, H. G. Dosch, V. I. Schevchenko, Yu. A. Simonov, Phys. Rep. 372 (2002) 319.

[28] Yu. A.Simonov, M. A. Trusov, JETP Lett. 85 (2007) 598.

[29] Yu. A.Simonov, M. A.Trusov, Phys. Lett. B650 (2007) 36.

[30] V. D. Orlovsky, Yu. A. Simonov, Phys. Rev. D89 (2014) 054012.

[31] M. Baldo, G. F. Burgio, P. Castorina, S. Plumari, D. Zappalà, Phys. Rev. D78 (2008) 063009.

[32] G. F. Burgio, M. Baldo, P. Castorina, S. Plumari, D. Zappalà, 8th Conference Quark Confinement and the Hadron Spectrum, September 1-6 2008, Mainz, Germany.

[33] S. Plumari, G. F. Burgio, V. Greco, D. Zappalà, Phys. Rev. D88 (2013) 083005.

[34] P. Castorina, V. Greco, S. Plumari, Phys. Rev. D92 (2015) 063530.

[35] I. Bombaci,D. Logoteta, Month. Not. Roy. Ast. Soc. 433 (2013) L79.

[36] D. Logoteta, I. Bombaci, Phys. Rev. D88 (2013) 063001.

[37] D. Logoteta, I. Bombaci, Journal of Physics: Conference Series 527 (2014) 012021.

[38] F. I. M. Pereira, Nucl. Phys A860 (2011) 102.

[39] F. I. M. Pereira, Nucl. Phys A897 (2013) 151.

[40] O.Kaczmarek, F. Zantov, arXiv:hep-lat/0506019.

[41] Yu. L. Vartanyan, A. K. Grigoryan, Astrophysics 42 (1999) 330.

[42] Yu. L. Vartanyan, A. K. Grigoryan, Astrophysics 44 (2001) 382.

[43] T. Lu, ASP Conference Series 138 (1998) 215.

[44] K. Hurley, T. Cline, E. Mazets, S. Barthelmy, P. Butterworth, F. Marshall, D. Palmer, R. Aptekar, S. Golenetskii, V. Il'Inskii, D. Frederiks, J. McTiernan, R. Gold, J. Trombka, Nature 397 (1999)41.

[45] S. L. Shapiro, S. A. Teukolsky, Black Holes, White Dwarfs and Neutron Stars, John Wiley and Sons, New York, 1983.

[46] N. Glendenning, Compact Stars, Nuclear Physics, Particle Physics, and Relativity, Springer, New York, 2000, 2nd ed..

[47] Ya. B. Zel'dovich and I. D. Novikov, Stars and Relativity, Dover Publications, Inc., Mineola, New York, 1996.

[48] B. K. Harrison, K. S. Thorn, M. Wakano, J. A. Wheeler, Gravitation Theory and Gravitational Collapse, University of Chicago Press, 1965.

[49] Yu. L. Vartanyan, A. R. Arutyunyan, A. K. Grigoryan, Astrophysics 37 (1994) 271.

[50] Yu. L. Vartanyan, A. K. Grigoryan, G. A. Khachatryan, Astrophysics 38 (1995) 152.

[51] Z. Berezhiani, I. Bombaci, A. Drago, F. Frontera, A. Lavagno, Astrophys. J. 586 (2003) 1250.

[52] B. L. Ioffe, K. Zyablyuk, Eur. Phys. J. C27 (2003) 229.

[53] T. A. S. do Carmo, G. Lugones, Physica A392 (2013) 6536.

[54] S. H. Kahana, J. Cooperstein, E. Baron, Phys. Lett. B196 (1987) 259.

[55] W. D. Arnet, J. N. Bachall, R. P. Kirshner, S. E. Woosley, Ann. Rev. Astron. Astrophys. 27 (1989) 629.

[56] S. R. Kulkarni S. G. Djorgovski, A. N. Ramaprakash, R. Goodrich, J. S. Bloom, K. L. Adelberger, T. Kundic, L. Lubin, D. A. Frail, F. Fronterak, M. Feroci, L. NicastroI, A. J. Barth, M. Davis, A. V. Filippenko, J. Newman, Nature 393 (1998) 35.

[57] R. Ouyed, J. Dey, M. Day, Astron. Astrophys. 390 (2002) L39.

[58] Kluzniak, W., Astron. Astrophys. 286 (1994) L17.

[59] R. R. Caldwell, J. L. Friedman, Phys. Lett. B264 (1991) 143.

[60] J. Sandweiss, RHIC News, https://www.bnl.gov/rhic/news/110607/story1.asp

[61] B. I. Abelev et al., STAR Collaboration, Phys. Rev. C76(2007)011901.

[62] M. Bleicher, F.M. Liu, J. Aichelin, H. J. Drescher, S. Ostapchenko, T. Pierog and K. Werner, Phys. Rev. Lett. 92(2004)072301.

[63] I. Bombaci, Journal of Physics: Conference Series 50 (2006) 208.

[64] X. D. Li, I. Bombaci, M. Dey, J. Dey, E. P. J. van den Heuvel, Phys. Rev. Lett. 83 (1999)3776.

[65] P. Haensel, A. Y. Potekhin, D. G. Yakovlev, Neutron Stars 1: Equation of State and Structure, Sringer, New York, 2007.

[66] R. X. Xu, Month. Not. Roy. Ast. Soc. 356 (2005) 359.

[67] R. X. Xu, Chin. J. Astron. Astrophys. 3 (2003) 33.

[68] F. I. M. Pereira, in progress.

FIGURE CAPTION

Fig. 1 - For the given values of G_2 (in GeV^4 units) and V_1 (in GeV units): panel (a) - gravitational mass M (solid line), baryonic mass M_A (short dashed line) and proper mass M_P (long dashed line) as functions of the central density. Labels 1 and 2 indicate the points at which $M = M_A$, where the solid line and short dashed line cross itself. Panel (b): M (solid line) and M_A (dashed line) as functions of the baryonic number N_A. Panel (c): mass defect as function of M. In panels (b) and (c) the labels 1 and 2 correspond to the ones in panel (a). All masses in units of the solar mass $M_\odot$.

Fig. 2 - As in Fig. 1, but for different values of G_2 and V_1 from top to bottom; each row with the same values of G_2 and V_1 from left to right.

Fig. 3 - The G_2 - V_1 plane showing the different regions according to the sign of $\Delta_2 M$. Region A: $\Delta_2 M > 0$ everywhere on the sequence of strange star configurations, as in panel (c) of Fig. 2. Region B: sequences with $\Delta_2 M \geq 0$ in the second branch and $\Delta_2 M < 0$ in the first branch or in both first branch and third branch, as in panel (c) of Fig. 1. Region C: $\Delta_2 M < 0$ everywhere on the sequence, as in panel (i) of Fig. 2. The upper curve corresponds to $\Delta_2 M = 0$ at the maximum mass of the sequence, as in panel (f) of Fig. 2 (cf. Fig. 6 in Ref. [38]). The lower curve corresponds to the limit between the regions A and B, where $\Delta_2 M = 0$ at the first endpoint as in panel (c) of Fig. 2, or both first endpoint and second endpoint of the sequence.

Fig. 4 - Panel (a): For several values of V_1, the mass defect at the maximum mass of the sequence of stellar configurations as function of G_2. Each curve is labeled by the value of V_1 (in GeV units) ranging from zero to 0.5 GeV. Panel (b): As in panel (a), but for values of G_2 extended up to $0.1\,\mathrm{GeV}^4$. The open circles at the upper part of the $V_1 = 0$ curve correspond to some values of B (in $\mathrm{MeV\,fm}^{-3}$) extracted from the literature between $B = 50$ $\mathrm{MeV\,fm}^{-3}$ and $B = 70$ $\mathrm{MeV\,fm}^{-3}$ [12–14, 49, 50], $B = 109$ $\mathrm{MeV\,fm}^{-3}$ [15], and $B = 208$ $\mathrm{MeV\,fm}^{-3}$ and $B = 508$ $\mathrm{MeV\,fm}^{-3}$ [51]. Along the $V_1 = 0$ curve and at $\Delta_2 M = 0$ is our calculated value of $\Delta|\varepsilon_{\mathrm{vac}}| = B = 170$ $\mathrm{MeV\,fm}^{-3}$ corresponding to $G_2 = 0.00927\,\mathrm{GeV}^4$.

Fig. 5 - Comparison between mass defects taking $m_A = m_n$ and $m_A = m_0$.

Fig. 6 - Panel (a): SQM stability windows at zero temperature and pressure, bounded by the $E/A = 0.9304\,\mathrm{GeV}$ (solid) contour of ${}^{56}F_{\mathrm{e}}$ and its vertical (dashed) line, for different choices of V_1 (in GeV units) labeling each contour (cf. panel (a) of Fig. 3 in Ref. [39]). Along the horizontal straight (dashed) line, the width of the stability window is the distance

from the vertical line to the corresponding E/A contour at a given V_1. Panel (b): The relative SQM stability as function of V_1 estimated according to three different ways. For each value of V_1: (solid line) the width of the stability window at $m_s = 0.15\,\mathrm{GeV}$ divided by the one at $m_s = 0$ (at the same V_1); (short dashed line) the width of the stability window at $m_s = 0.15\,\mathrm{GeV}$ divided by the one at $V_1 = 0$ (at the same $m_s = 0.15\,\mathrm{GeV}$); (long dashed line) the width of the stability window at $m_s = 0.15\,\mathrm{GeV}$ divided by the largest one (at $V_1 = 0$ and $m_s = 0$) .

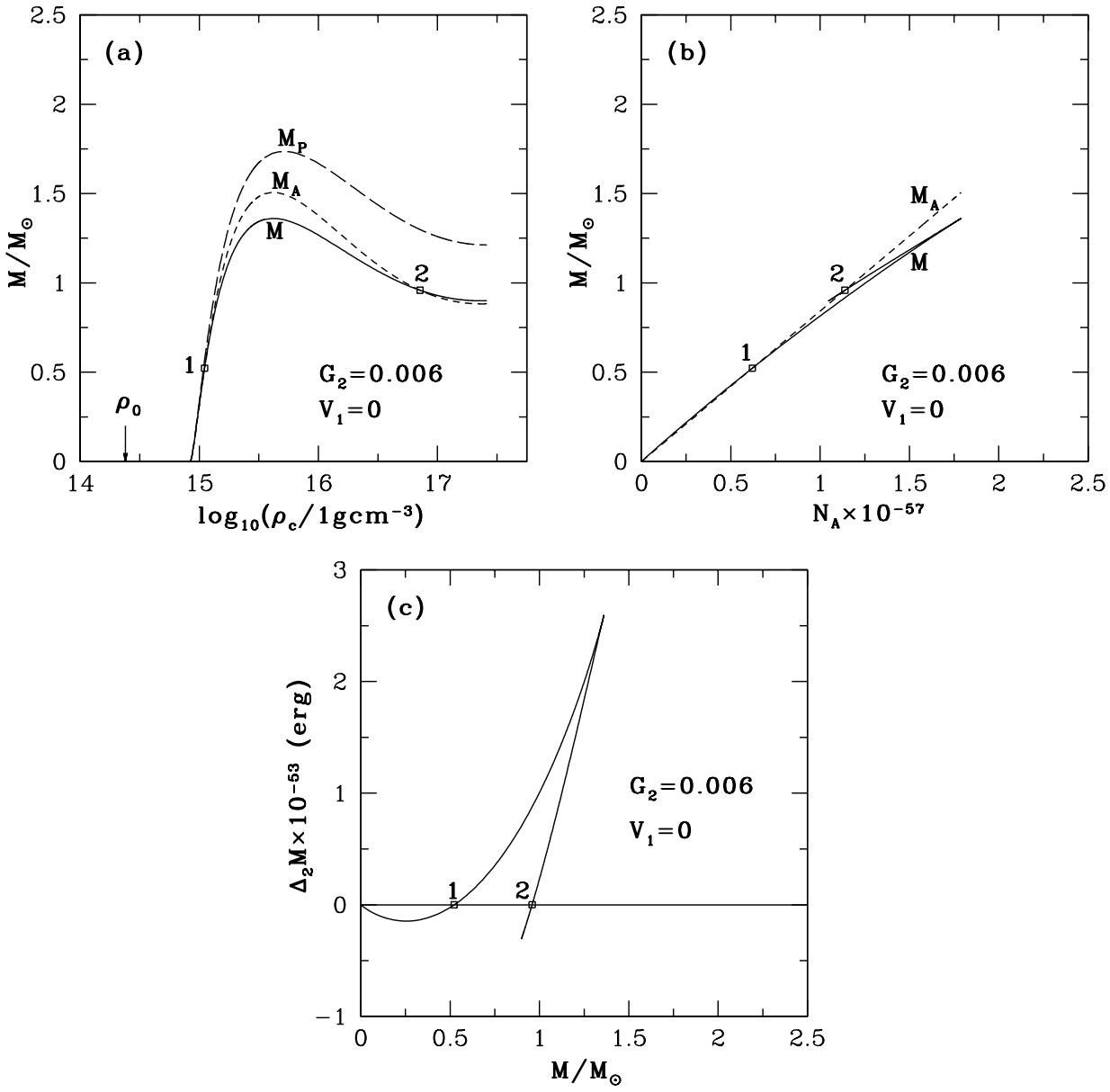
(a)
M/M⊙
log10(ρc/1gcm−3)
MP
MA
M
1
2
ρ0
G2=0.006
V1=0
(b)
M/M⊙
NA×10−57
MA
M
1
2
G2=0.006
V1=0
(c)
Δ2M×10−53 (erg)
M/M⊙
1
2
G2=0.006
V1=0

FIG. 1:

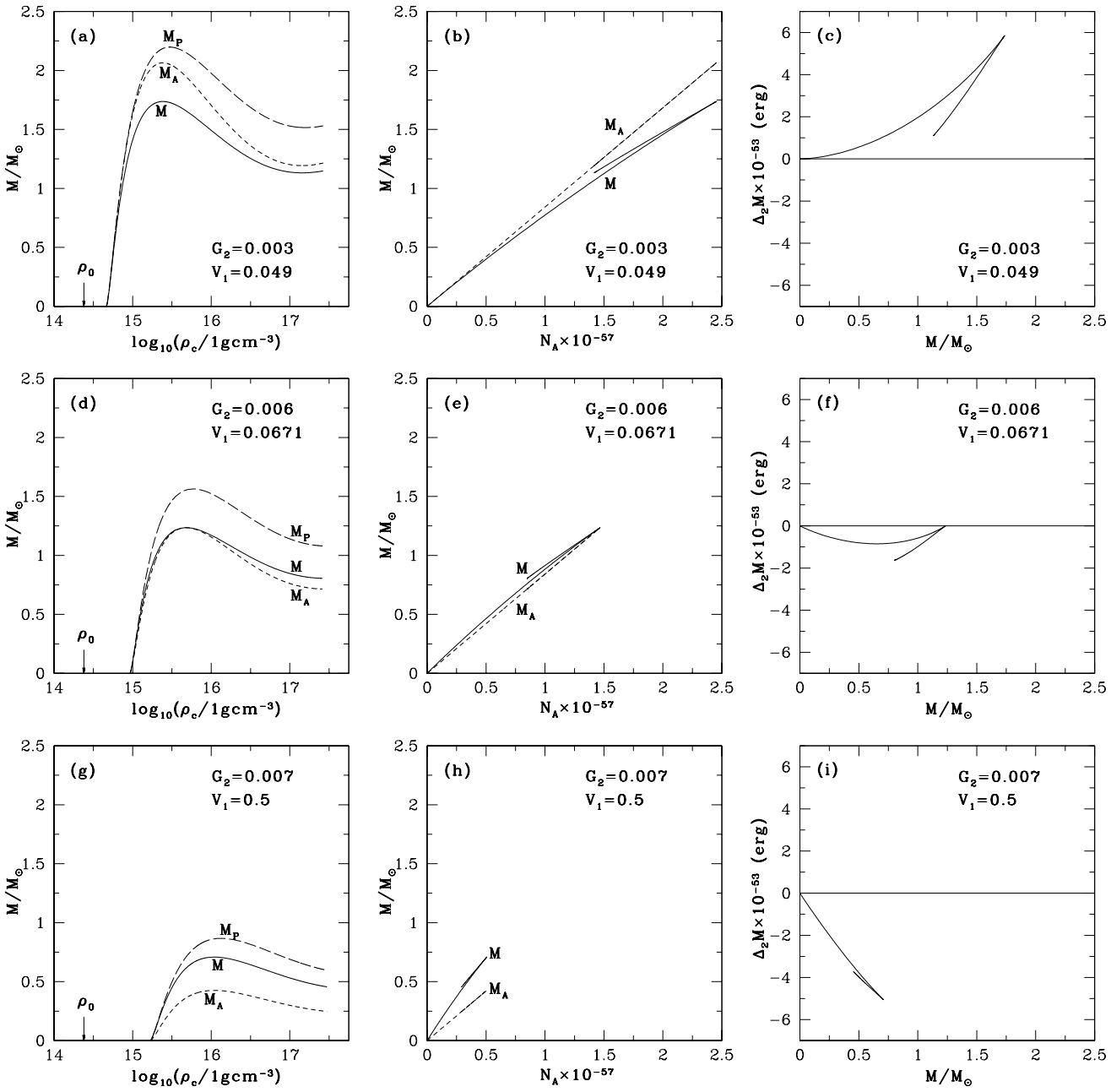
(a)
M_P
M_A
M
G_2=0.003
V_1=0.049
ρ_0
$M/M_\odot$
$\log_{10}(\rho_c/1gcm^{-3})$
(b)
M_A
M
G_2=0.003
V_1=0.049
$M/M_\odot$
$N_A\times10^{-57}$
(c)
G_2=0.003
V_1=0.049
$\Delta_2M\times10^{-53}$ (erg)
$M/M_\odot$
(d)
G_2=0.006
V_1=0.0671
M_P
M
M_A
ρ_0
$M/M_\odot$
$\log_{10}(\rho_c/1gcm^{-3})$
(e)
G_2=0.006
V_1=0.0671
M
M_A
$M/M_\odot$
$N_A\times10^{-57}$
(f)
G_2=0.006
V_1=0.0671
$\Delta_2M\times10^{-53}$ (erg)
$M/M_\odot$
(g)
G_2=0.007
V_1=0.5
M_P
M
M_A
ρ_0
$M/M_\odot$
$\log_{10}(\rho_c/1gcm^{-3})$
(h)
G_2=0.007
V_1=0.5
M
M_A
$M/M_\odot$
$N_A\times10^{-57}$
(i)
G_2=0.007
V_1=0.5
$\Delta_2M\times10^{-53}$ (erg)
$M/M_\odot$

FIG. 2:

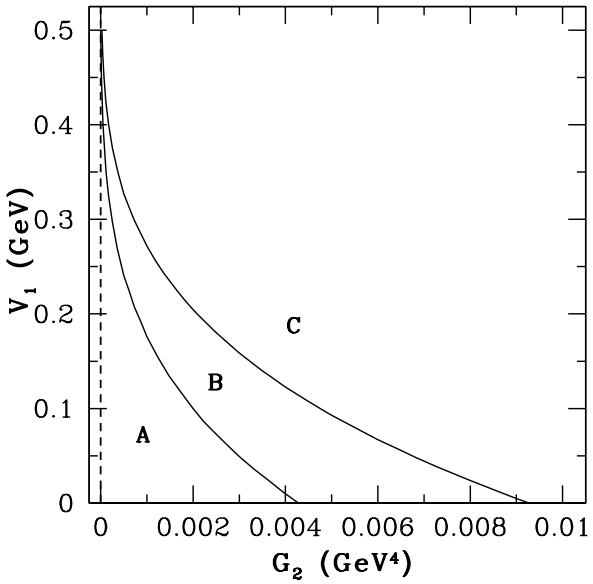

FIG. 3:

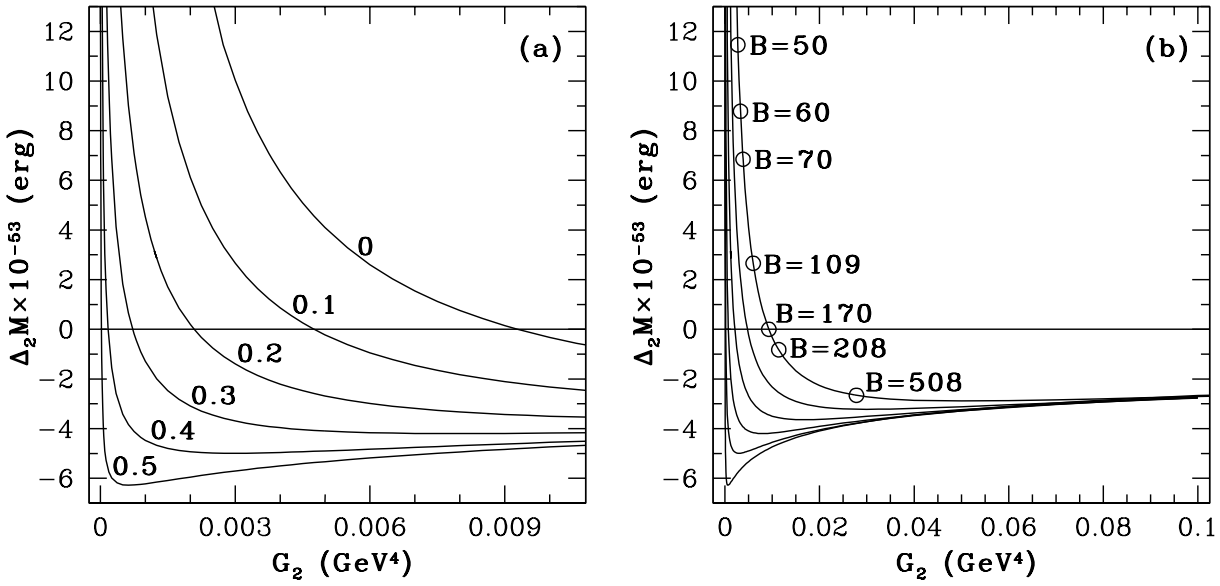
(a)
(b)
$\Delta_2 M \times 10^{-53}$ (erg)
G_2 (GeV^4)
0
0.1
0.2
0.3
0.4
0.5
B=50
B=60
B=70
B=109
B=170
B=208
B=508

FIG. 4:

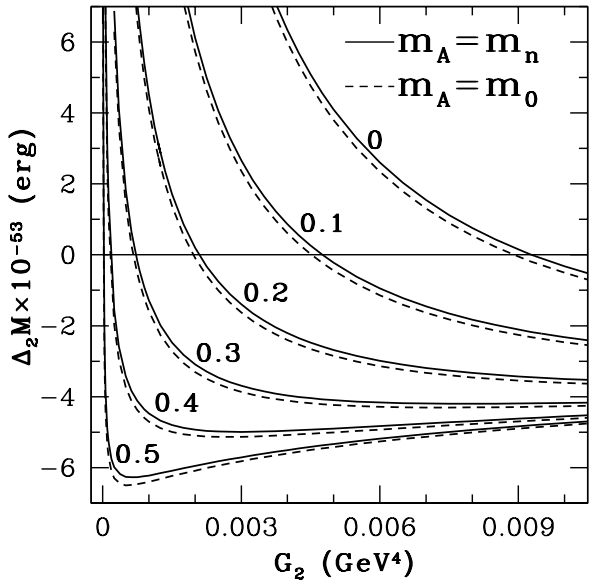
$m_A = m_n$
$m_A = m_0$
0
0.1
0.2
0.3
0.4
0.5
$\Delta_2 M \times 10^{-53}$ (erg)
G_2 (GeV^4)
6
4
2
0
−2
−4
−6
0
0.003
0.006
0.009

FIG. 5:

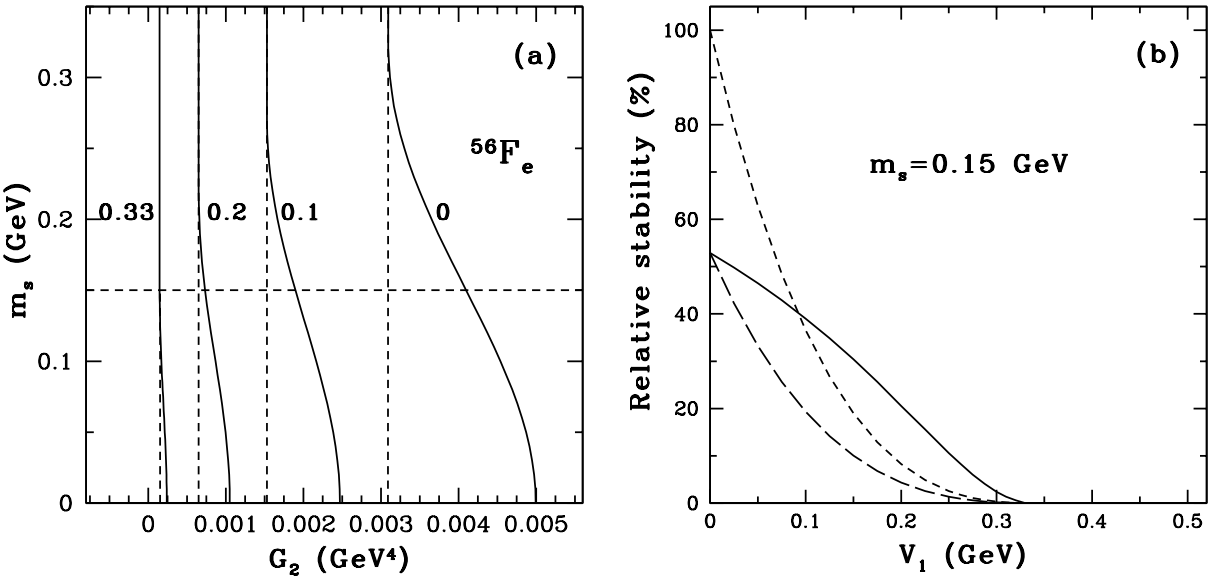
(a)
$^{56}F_e$
0.33
0.2
0.1
0
m_s (GeV)
G_2 (GeV^4)
(b)
m_s=0.15 GeV
Relative stability (%)
V_1 (GeV)

FIG. 6: